

# Properties of quasi two-dimensional condensates in highly anisotropic traps

G. Hechenblaikner, J. M. Krueger, and C. J. Foot  
*Clarendon Laboratory, Department of Physics, University of Oxford,  
Parks Road, Oxford, OX1 3PU,  
United Kingdom.*

(Dated: October 12, 2018)

We theoretically investigate some of the observable properties of quasi two-dimensional condensates. Using a variational model based on a Gaussian-parabolic trial wavefunction we calculate chemical potential, condensate size in time-of-flight, release energy and collective excitation spectrum for varying trap geometries and atom numbers and find good agreement with recent published experimental results.

## I. INTRODUCTION

Bose-Einstein condensation of dilute atomic gases has been achieved in a variety of magnetic and optical dipole force traps with different geometries. There is considerable interest in studying the properties of these ultra-cold gases under conditions where the confinement gives a system with dimensionality less than 3; recent experiments in optical lattices have observed the properties of a one-dimensional Tonks gas [1] in which bosons show fermionic properties. Several other experiments have realised conditions of two-dimensional confinement, i.e. where one degree of freedom is frozen out [2], [3], [4]; however, the new physics in this regime remains to be explored: a two dimensional Bose gas in a homogenous potential does not undergo Bose-Einstein condensation (BEC), instead there is a Berenzinskii-Kosterlitz-Thouless transition (a topological phase transition mediated by the spontaneous formation of vortex pairs), a system that is superfluid even though it does not possess long-range order. This is counter the usual picture of superfluidity in three dimensions explained in terms of a macroscopic wavefunction describing the whole system. Early experiments on the KT transition were carried out with films of superfluid  $^4\text{He}$  [5][6] and more recent ones include the observation of quasi-condensates in thin layers of spin-polarized hydrogen [7].

In recent experiments, BECs created in conventional three-dimensional magnetic traps have been put into the quasi-2d (Q2D) regime through the addition of an optical potential. In this limit the interaction energy, proportional to the chemical potential  $\mu$ , is on the order of or smaller than the harmonic oscillator level spacing and along the tightly confined axial direction the characteristics of the condensate are those of an ideal gas. The crossover to the Q2D regime was first observed in [2] and in [3] by continuously removing atoms from a highly anisotropic trap to decrease the interaction energy. In the experiment described in [4] the Q2D crossover is observed by gradually increasing the trap anisotropy from moderate to very large values whilst keeping the number of atoms fixed.

The main aim of this paper is to use a simple theoretical model to examine some of the characteristic prop-

erties of Q2D condensates, e.g. the chemical potential, release energy and quadrupole mode spectra are each calculated for a variety of various trap anisotropies which are achieved in the experiments. Note that a similar variational approach was taken in [8] which investigates the crossover to lower dimensions in general. We extend and expand upon this analysis by making a more general ansatz for the trial wavefunction (breaking the axial symmetry) and deriving analytical expressions for chemical potential, total energy, release energy and radial condensate widths in the Q2D regime; a polynomial equation the solution of which gives the axial and radial condensate sizes in all regimes is also derived. It is used to calculate physical properties in all regimes and plot the crossover from the hydrodynamic to the Q2D limit for a number of physical quantities. The theoretical results are in very good agreement with the data of a recent experiment in [4]. We numerically calculate the frequency spectrum for the lowest quadrupole modes and also find an approximate analytic expression.

The paper is structured as follows: In the second section we develop a formalism that allows us to calculate the ground state and the dynamics of a Q2D gas; starting from a Gaussian-parabolic trial wavefunction we use a variational method to obtain a set of differential equations for the dynamics of the Q2D condensate and a polynomial equation for the ground state. We then examine the criteria for Q2D and calculate the chemical potential and energy per particle across the hydrodynamic-Q2D crossover. In section IV we calculate the size and release energy of condensates in time-of-flight which are released from traps of varying anisotropy and make a quantitative comparison with recent experimental data [4]. The final section examines the change of collective excitation frequencies across the Q2D transition for the two quadrupole modes with zero angular momentum followed by the conclusions and a brief outlook.

## II. THE HYBRID VARIATIONAL MODEL

Condensates are usually trapped in harmonic potentials given by

$$V_{\text{ext}} = \frac{m}{2}\omega_0^2 \sum_i \lambda_i^2 x_i^2, \quad (1)$$

where the  $\lambda_i(t)$  denote the trap anisotropies which can in general depend on time. A quasi-2D trap has  $\lambda_z \gg \lambda_{x,y}$ . For large anisotropies the condensate shape along the z-direction is very similar to the Gaussian profile of an ideal gas. However, along the weakly confined x- and y-axes the condensate has a parabolic shape characteristic of the hydrodynamic regime. The best description in terms of simple analytic functions is therefore to model the condensate wavefunction as a hybrid of parabola and Gaussian. Experiments on the condensate expansion in various regimes show the smooth crossover from hydrodynamic expansion to the characteristics of a quasi-2D gas, which essentially expands like an ideal non-interacting gas. To determine the dynamics of the quasi-2D condensate we use a variational method, as introduced in [9], and define the trial wavefunction

$$\psi = A_n \sqrt{1 - \frac{x^2}{l_x^2} - \frac{y^2}{l_y^2}} e^{-\frac{z^2}{2l_z^2}} e^{i(\beta_x x^2 + \beta_y y^2 + \beta_z z^2)}, \quad (2)$$

where the normalization constant  $A_n$  is given by

$$A_n^2 = \frac{2}{l_x l_y l_z \pi^{3/2}}. \quad (3)$$

The condensate width  $l_i(t)$  and phase  $\beta_i(t)$  parameters are functions of time and their time evolution completely describes that of the condensate. The condensate density profile is at all times restricted to a parabolic shape in the radial plane and a Gaussian shape along the highly compressed axial direction. The Lagrangian density for the nonlinear Schrödinger equation is given by

$$\begin{aligned} \mathcal{L} \equiv & \frac{1}{2}i\hbar \left( \frac{\partial\psi^*}{\partial t} \psi - \psi^* \frac{\partial\psi}{\partial t} \right) + \frac{\hbar^2}{2m} |\nabla\psi|^2 \\ & + V_{\text{ext}}(\mathbf{r}, t) |\psi|^2 + \frac{1}{2}gN |\psi|^4; \end{aligned} \quad (4)$$

with the nonlinearity parameter  $g = 4\pi\hbar^2 a/m$ , where  $a$  is the scattering length,  $N$  is the number of atoms in the condensate and  $m$  is the atomic mass. After inserting the trial wave-function (2) into Eq.(4) the corresponding Lagrangian is found through integration  $L = \int \mathcal{L} d^3x$ ; the four terms of Eq.(4) lead to

$$\begin{aligned} L = & L_1 + L_2 + L_3 + L_4 = \\ & \frac{\hbar}{2} \left( \frac{\dot{\beta}_x l_x^2}{3} + \frac{\dot{\beta}_y l_y^2}{3} + \dot{\beta}_z l_z^2 \right) + \\ & \frac{\hbar^2}{m} \left( \frac{\beta_x^2 l_x^2}{3} + \frac{\beta_y^2 l_y^2}{3} + \beta_z^2 l_z^2 + \frac{1}{4l_z^2} \right) + \end{aligned}$$

$$\begin{aligned} & \frac{m}{4} \left( \frac{\omega_x^2 l_x^2}{3} + \frac{\omega_y^2 l_y^2}{3} + \omega_z^2 l_z^2 \right) + \\ & \frac{\sqrt{2}gN}{3l_x l_y l_z \pi^{3/2}}, \end{aligned} \quad (5)$$

where we omitted the ‘quantum pressure’ term [10] for the  $x$  and  $y$  directions (where this term is divergent due to the sharp boundaries of the condensate wavefunction in the hydrodynamic regime) but retained it for the  $z$ -direction where the condensate assumes the Gaussian shape of an ideal non-interacting gas (as the term proportional to  $1/l_z^2$ ). The quantum pressure term is crucial in describing the dynamics. The total energy per particle  $E_{\text{tot}}$  and the chemical potential  $\mu$  are given by

$$E_{\text{tot}} = E_{\text{kin}} + E_{\text{pot}} + E_{\text{int}} \quad \mu = E_{\text{kin}} + E_{\text{pot}} + 2E_{\text{int}}, \quad (6)$$

where  $E_{\text{kin}}$ ,  $E_{\text{pot}}$  and  $E_{\text{int}}$  are the kinetic, potential and interaction energy, given by the last three terms of the Lagrangian (5), respectively. The Euler Lagrange equations

$$\frac{d}{dt} \frac{\partial L}{\partial \dot{l}_i} = \frac{\partial L}{\partial l_i}, \quad \frac{d}{dt} \frac{\partial L}{\partial \dot{\beta}_i} = \frac{\partial L}{\partial \beta_i}. \quad (7)$$

yield the dynamic equations for the condensate widths  $l_i$  and phases  $\beta_i$ . We find for the widths

$$\dot{l}_i = \frac{2\hbar}{m} \beta_i l_i. \quad (8)$$

After differentiating Eqs. (8) once more w.r.t. time one can express the resulting second order equation in terms of the  $l_i$  alone:

$$\ddot{l}_i = -\omega_i^2(t) l_i + \left( \frac{2}{\pi} \right)^{\frac{3}{2}} \frac{gN}{m} \frac{1}{l_i l_x l_y l_z} \left( 1 - \frac{2}{3} \delta_{iz} \right) + \frac{\hbar^2}{m^2} \frac{1}{l_i^3} \delta_{iz}, \quad (9)$$

where  $\delta_{iz} = 1$  for  $i = z$  and 0 otherwise. It is convenient to express the above equation in dimensionless quantities, so we introduce the dimensionless time  $\tau$  and widths  $d_i$  defined by

$$d_i = \frac{l_i}{a_0}, \quad \tau = t\omega_0, \quad (10)$$

where  $a_0 = \sqrt{\hbar/(m\omega_0)}$  is the harmonic oscillator length. In terms of these quantities Eq.(10) can be rewritten as

$$\ddot{d}_i = -\lambda_i^2(t) d_i + \frac{C_p}{d_i d_x d_y d_z} \left( 1 - \frac{2}{3} \delta_{iz} \right) + \frac{1}{d_z^3} \delta_{iz}, \quad (11)$$

where the constant  $C_p = 8\sqrt{\frac{2}{\pi}} \frac{a}{a_0} N$ . To find the ground state of Eqs.(11) we have to set the left side equal to zero and solve the remaining coupled nonlinear equations:

$$d_{i0}^2 \lambda_{i0}^2 = \frac{C_p}{d_{x0} d_{y0} d_{z0}} \left( 1 - \frac{2}{3} \delta_{iz} \right) + \frac{1}{d_{z0}^2} \delta_{iz}. \quad (12)$$

This cannot be done analytically but it is straight forward to find a numerical solution. After some algebra and using various symmetries the three coupled equations can be reduced to one polynomial equation. Introducing new dimensionless units  $D_i$ , defined as the condensate widths  $l_i$  normalized by the axial harmonic oscillator length  $a_z$ , i.e.  $D_i = l_i/a_z$ , the polynomial equation can be written as

$$\gamma^8 = \frac{1}{3} \left( \frac{C_p \lambda_{x0} \lambda_{y0}}{\lambda_z^{3/2}} \right)^{1/2} \gamma^3 + 1, \quad (13)$$

where  $D_z = \gamma^2$ . There is only one real and positive solution to this equation For the x- and y widths we find

$$D_x = \left( \frac{C_p \lambda_{y0} \lambda_{z0}^{5/2}}{D_z \lambda_{x0}^3} \right)^{1/4}, \quad D_y = D_x \frac{\lambda_{x0}}{\lambda_{y0}}. \quad (14)$$

### III. CRITERIA FOR QUASI-2D

We shall now examine the case where the anisotropy becomes very large. A solution to Eq.(13) is then given by neglecting the first term on the r.h.s. and solving the remaining equation. We find that  $\gamma^2 = D_z = 1$  and thus the approximate solution is given by the axial harmonic oscillator length

$$l_{z0} = \sqrt{\frac{\hbar}{m\omega_z}}. \quad (15)$$

It is the minimum width the condensate shape can attain and it is also the solution for the width of a non-interacting gas. For this reason the gas along the z-direction is said to have the characteristics of an ideal non-interacting gas. We will see that this also applies to the expansion and the collective excitations of the gas which become identical to those of an ideal gas in the limit of large anisotropies.

It is interesting to examine the range of validity of this approximation and find an estimate of the error. Demanding that the first term on the r.h.s. of Eq.(13) is much smaller than the second we see that the error or the deviation from the ideal gas solution scales with the ratio of  $N\lambda_{x0}\lambda_{y0}/\lambda_{z0}^{3/2}$ . The 2D-regime can be reached by either decreasing the number or increasing the axial frequency.

Now we calculate the chemical potential from Eq.(6) and the terms of the Lagrangian (5) and obtain after some algebra

$$\tilde{\mu} = \frac{1}{2} m \omega_x^2 l_{x0}^2, \quad \tilde{\mu} = \mu - \frac{\hbar\omega_z}{2}, \quad (16)$$

where we used  $\omega_x^2 l_{x0}^2 = \omega_y^2 l_{y0}^2$ , the expression for  $l_{z0}$  (Eq. 15) and other symmetries of Eqs.(12). We find that the relation  $l_i = \sqrt{2\tilde{\mu}/m\omega_i^2}$ ,  $i = x, y$  is similar to that of a hydrodynamic gas [11], only that for the quasi-2D gas we

use the chemical potential shifted by an amount  $\hbar\omega_z/2$  to calculate the radial width. Inserting solution (15) for the axial width into Eq. (14) we obtain explicit expressions for the radial width

$$l_{x0}^2 = a_0^2 \left( 8\sqrt{\frac{2}{\pi}} N \frac{a}{a_0} \frac{\lambda_{y0} \lambda_{z0}^{1/2}}{\lambda_{x0}^3} \right)^{\frac{1}{2}} \quad (17)$$

and, after substituting into Eq. (16), for the chemical potential

$$\mu = \frac{\hbar\omega_z}{2} \left[ 1 + \left( 8\sqrt{\frac{2}{\pi}} N \frac{a}{a_0} \frac{\lambda_{x0} \lambda_{y0}}{\lambda_{z0}^{3/2}} \right)^{\frac{1}{2}} \right]. \quad (18)$$

This expression shows that the chemical potential tends towards  $\hbar\omega_z/2$ , the harmonic oscillator ground state energy, which is the energy per particle and also the chemical potential of the ideal non-interacting gas. The deviation from this value is small for a quasi-2D gas, and interestingly, given by the same value as the correction to the axial condensate width of Eq.(13). Note, however, that this small deviation is vital for consistency. It is proportional to the square of the radial condensate width (see Eq. 16). If it was zero the radial condensate width would also be zero which is neither possible nor self consistent. The expression for the Q2D chemical potential should be compared to that of a 3D hydrodynamic gas  $\mu_{3D}$  for which we obtain from [11] after some rearrangements

$$\mu_{3d} = \left( 15N \frac{a}{a_0} \frac{\lambda_{x0} \lambda_{y0}}{\lambda_{z0}^{3/2}} \right)^{\frac{2}{5}}. \quad (19)$$

We observe that this expression tends towards zero for  $N \rightarrow 0$  and the power law is also different from the Q2D expression (18). In previous papers [2] the condition  $\mu_{3D} < \hbar\omega_z$  was listed as a criterion for Q2D as  $\mu_{3D}$  is on the order of the interaction energy at low densities. Similarly we can impose the condition  $\mu < \hbar\omega_z$  on the expression of the Q2D chemical potential of Eq. (18) and we find for the maximum number of atoms to achieve 2D for a given trap geometry

$$N < C \sqrt{\frac{\hbar}{ma^2}} \sqrt{\frac{\omega_z^3}{\omega_x^2 \omega_y^2}}, \quad (20)$$

where the constant  $C = \sqrt{32/225}$  for  $\mu_{3D} < \hbar\omega_z$  and  $C = \sqrt{\pi/256}$  for  $\mu < \hbar\omega_z$ .

In Fig. 1a we show plots of the chemical potential as a function of increasing radial trap frequency  $\omega_r = \omega_x = \omega_y$ , whereas the axial frequency remains constant at  $\omega_z/2\pi = 2.2$  kHz and the number of atoms is taken to be  $N = 8 \times 10^4$ . For very small values of  $\omega_r$  the anisotropy  $A = \lambda_z/\lambda_x$  is very high and the chemical potential approaches  $\mu = \hbar\omega_z/2$ . Gradually increasing the radial trap frequency has the effect of reducing the anisotropy

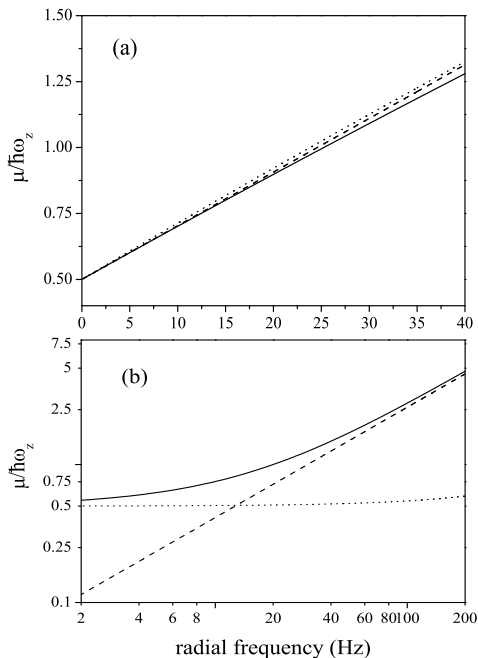


FIG. 1: (a) The chemical potential plotted in units of  $\hbar\omega_z$  against increasing radial trap frequency: hybrid variational model (solid line), analytic approximation (dashed line), Gaussian variational model (dotted line); (b) the chemical potential plotted for a wider range of radial trap frequencies; the ideal gas limit is given by the dotted line, the hydrodynamic prediction by the dashed line.

and increasing the chemical potential. An exact numerical solution using the variational hybrid model is given by the solid line. The dashed line denotes the analytical approximation as given by Eq. (18) for a condensate well in the Q2D regime. There is very good agreement between the two for frequencies up to  $\omega_r \simeq 20$  Hz, where the anisotropy is on the order of  $A \simeq 100$  and  $\mu \approx \hbar\omega_z$ . The dotted line is given by the results of a Gaussian variational model as described in [9], where the trial wavefunction in all spatial directions is given by a Gaussian. It is remarkable how similar the results are for both models. In physical reality the actual wavefunction in the radial direction should be close to the inverted parabola we use in our ‘hybrid model’ (see Eq.2). The plot in Fig. 1b shows the chemical potential for a wider range of radial frequencies  $\omega_r$  (solid line) on logarithmic scales; this shows how the values bend from the hydrodynamic asymptote (dashed line) to the ideal gas value of  $\hbar\omega_z/2$  (dotted line), with the bending point given by values of  $\omega_r/2\pi \approx 20$  Hz and  $\mu \approx \hbar\omega_z$ . From Eqs. (5,6,16) we find the following useful relations between the various energy

contributions to the Lagrangian:

$$E_{\text{kin}} = \frac{\hbar\omega_z}{4} = E_{\text{pot}}^z, \quad E_{\text{pot}}^x = E_{\text{pot}}^y = \frac{E_{\text{int}}}{2} \quad (21)$$

Using Eq.(6) the total energy per particle is found from the Lagrangian (5) to be

$$E_{\text{tot}} = \frac{\hbar\omega_z}{2} + \frac{m\omega_x^2 l_{x0}^2}{3} = \frac{\hbar\omega_z}{2} + \frac{2}{3}\tilde{\mu}. \quad (22)$$

For large anisotropies and small atom numbers this expression tends towards  $\hbar\omega_z/2$ , the harmonic oscillator ground state energy. This is what we expected, given that in the Q2D regime the gas is non-interacting and thus the energy per particle is equal to the chemical potential. The release energy, defined as the energy of the expanding cloud once the trap has been switched off, is given by the sum of the in-trap kinetic and interaction energies:

$$E_{\text{rel}} = E_{\text{kin}} + E_{\text{int}} = \frac{\hbar\omega_z}{4} + \frac{1}{3}\tilde{\mu} = \frac{E_{\text{tot}}}{2}, \quad (23)$$

which tends toward  $\hbar\omega_z/4$ , equal to half the ground state energy, because the potential energy was lost when the atoms were released from the trap. We also find the atomic peak density  $n_{\text{peak}}$  of the Q2D distribution, given by Eq. (2), from Eqs. (3,15,17):

$$n_{\text{peak}} = NA_n^2 = \frac{\tilde{\mu}}{g} = \left( \frac{N}{(2\pi)^{\frac{5}{2}}} \frac{\lambda_{x0}\lambda_{y0}\lambda_{z0}^{\frac{1}{2}}}{a_0^5 a} \right)^{\frac{1}{2}}. \quad (24)$$

#### IV. CONDENSATE EXPANSION AND RELEASE ENERGY

It is interesting to examine the expansion of the condensate in time-of-flight (TOF) in the 2D-regime. As a Q2D gas resembles an ideal gas in the axial direction its expansion is described by the Schrödinger equation and can be calculated analytically. Looking at Eqs. (9), noting that  $\lambda_z(t) = 0$  for expansion and neglecting the second term describing the interaction we obtain  $\ddot{l}_z = \hbar^2/(m^2 l_z^3)$ . The solution to this second order differential equation for  $l_z(0) = l_{z0}$  and  $\dot{l}_z = 0$  is given by

$$l_z = l_{z0} \sqrt{1 + \frac{\hbar^2 t^2}{m^2 l_{z0}^4}} = l_{z0} \sqrt{1 + \omega_z^2 t^2}, \quad (25)$$

where Eq. (15) has been used. In the following we will refer to this simple expression as the ‘ideal gas expansion’. Fig. 2 shows the axial and radial condensate widths, normalized by their initial values (in the trap), during TOF for a trap with  $N = 8 \times 10^4$  atoms,  $\omega_z/2\pi = 2.2$  kHz and  $\omega_r/2\pi = 7$  Hz, which are typical parameters for the experiment in [4]. The prediction of the hybrid model, which is indistinguishable from that of the Gaussian variational model, is given by the solid line. For the axial direction, shown in (a), it is very close to the expansion of

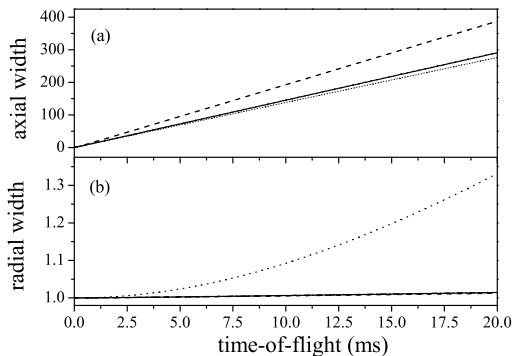


FIG. 2: The condensate axial (a) and radial (b) widths, normalized by their initial values, plotted in TOF. The solid line is based upon the hybrid model, the dotted upon the expansion of a non-interacting wavepacket and the dashed line upon the hydrodynamic theory.

the ideal gas given by Eq. (25) and plotted as the dotted line. The faster expansion of a hydrodynamic gas [12] is given by the dashed line. These curves demonstrate clearly that for the axial expansion the system behaves like an ideal gas. This contrasts the radial expansion of Fig. 2b, where the hybrid and Gaussian variational models (solid line) agree nearly perfectly with the hydrodynamic theory (dashed line) but are far removed from the ideal gas expansion (dotted line); this demonstrates the hydrodynamic character of the radial expansion.

In Fig. 2 we plotted the condensate expansion as a function of time; however, in the experiment in [4] the expansion times are kept constant at 15 ms and the radial trap frequency  $\omega_r$  is varied to explore the various regimes and the crossover to Q2D. The measurements in [4] were done for two different axial trap frequencies and atom numbers. The results of the measurements are shown in Fig. 3a, where the open and filled circles are the data for traps in which the atoms initially have axial oscillation frequencies of  $\omega_z/2\pi = 1990$  Hz and 960 Hz, respectively. To obtain a theoretical comparison we propagate the hybrid model Eqs. (11) repeatedly for varying initial conditions obtained from Eq. (13). The hybrid model predictions for the two optical traps are given by the solid lines and we find good agreement to the experimental data for both traps. The horizontal dashed lines indicate the expansion of the ideal gas, given by Eq. (25) and the dotted lines the expansion of the hydrodynamic gas. The ‘ideal gas’ and hydrodynamic models yield straight lines on the log-log plot. In contrast, the curve for the hybrid model follows the hydrodynamic asymptote down to  $\omega_r \approx 20$  Hz, corresponding to  $\mu \approx \hbar\omega_z$ , where it bends and follows the ‘ideal gas’ line towards zero radial frequency. This transition from the hydrodynamic to the ‘ideal gas’ asymptote gives conclusive evidence of the gas entering the Q2D regime. There is a noticeable deviation for  $\omega_r$  well below the cross-over frequency because

in the experiment imperfections broke the radial symmetry and added a residual potential along the y-axis. This was taken into account in the theoretical calculations. There is good agreement with the experimental data. The overall frequencies in x- and y-direction are given by  $\omega_x = \omega_r$  and  $\omega_y = \sqrt{\omega_r^2 + (\omega_y^{\text{res}})^2}$ . The residual frequencies  $\omega_y^{\text{res}}$  were measured in [4] and are given by  $\omega_y^{\text{res}}/2\pi = 26$  Hz for the trap with  $\omega_z/2\pi = 1990$  Hz and  $\omega_y^{\text{res}}/2\pi = 12$  Hz for the trap with  $\omega_z/2\pi = 960$  Hz.

It is also possible to calculate the release energy  $E_{\text{rel}}$  of the condensate from the experimental measurements of its axial width as has been done in [2]. The release energy is easily calculated after a long time-of-flight. In this case the potential term in Eq. (6b) is zero and the interaction term negligible so that we are left with the kinetic energy alone and find  $E_{\text{rel}} = E_{\text{kin}}$ . The terms in x and y can be neglected as most energy is in the previously tightly confined z-direction and we obtain from the Lagrangian (5) an expression for the release energy

$$E_{\text{rel}} \approx E_{\text{kin}}^z \approx \frac{\hbar^2}{m} \left( l_z^2 \beta_z^2 + \frac{1}{4l_z^2} \right) = \frac{m}{4} \dot{l}_z^2 + \frac{1}{4} \frac{\hbar^2}{m} \frac{1}{l_z^2}, \quad (26)$$

where we used relation (8) for the last step. After an initial acceleration, when released from the trap, the condensate moves with constant velocity and after long enough time-of-flight (TOF) we can approximate  $\dot{l}_z \approx l_z/t$ , where t is the TOF. The release energy is then written as

$$E_{\text{rel}} \approx \frac{m}{4} \frac{l_z^2}{t^2}, \quad (27)$$

where we neglected the quantum pressure proportional to  $1/l_z^2$  as it tends to zero for long time-of-flights. In a Q2D gas the total energy is given by the sum of the potential and the kinetic energy in the axial direction, both of which contribute by an equal amount to the harmonic oscillator ground state. As the potential energy is lost when the trap is switched off the remaining kinetic energy constitutes half the ground state energy so that  $E_{\text{rel}} = \hbar\omega_z/4$ . The release energies for the same set of data as in (a) are plotted in Fig. 3b, Eq.(27) was used to determine the release energy from the condensate width. The theoretical predictions of the hybrid model are given by the solid lines, the dashed lines indicate the value for the ground state and the first excited state, respectively. In [2] the expression  $E_{\text{rel}}^p = mL_z^2/(14t^2)$  is used to find the release energy, where  $L_z$  is the width of a fitted inverted parabola. This formula can be derived by making a fully parabolic ansatz to the trial wavefunction - an approach that is valid in the hydrodynamic limit but is not really applicable in the Q2D limit, where one should rather use Eq. (27) as otherwise the release energy is underestimated by about 20%.

There is excellent agreement between the theoretical predictions and the experimental data and we find that the release energy does indeed go towards  $\hbar\omega_z/4$  indicating that the Q2D limit was reached in the experiment [4].

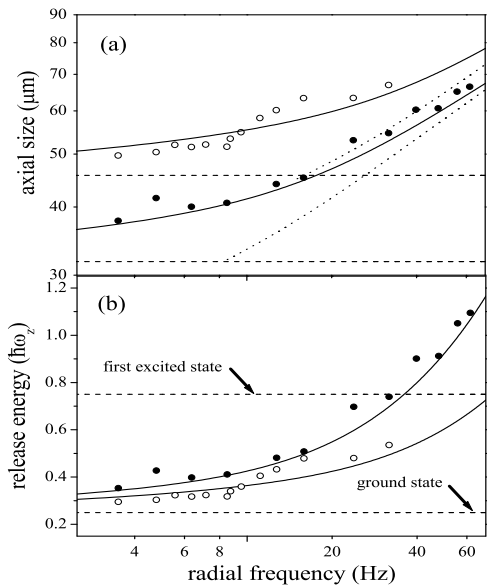


FIG. 3: (a) The axial expansion of the condensate in TOF for two different trap geometries and atom numbers. Solid lines indicate the theoretical predictions, dashed lines indicate the ideal gas limit and dotted lines the hydrodynamic limit. The data are taken for traps with initial oscillation frequencies (before release) of  $\omega_z/2\pi = 1990$  Hz (open circles), 960 Hz (filled circles) [4]. The atom numbers are  $8 \times 10^4$  and  $1.1 \times 10^5$  for the upper and lower curves, respectively. (b) release energies for the same data points; the dashed lines indicate the energies of the ground and the first excited state.

## V. COLLECTIVE EXCITATIONS IN Q2D

Another, as yet unexplored, method to observe the transition to Q2D is to probe the collective excitation spectrum. An ansatz for the trial wavefunction of the type (2) allows for the description of the three quadrupolar modes [11]. In an axially symmetric trap they are given by the  $m = 2$  mode and the  $m = 0$  low- and high-lying modes, where  $m$  denotes the angular momentum quantum number. In order to calculate the mode frequencies we linearise the dynamic equations of the hybrid model (11) around the ground state. Making the ansatz

$$d_i = d_{i0} + \epsilon_i, \quad (28)$$

inserting it into Eqs.(11), expanding up to first order in  $\epsilon$ , and using Eqs.(12) to simplify and combine certain

terms, we obtain after some algebra

$$\begin{pmatrix} \ddot{\epsilon}_x \\ \ddot{\epsilon}_y \\ \ddot{\epsilon}_z \end{pmatrix} = - \begin{pmatrix} \frac{3C_p}{d_{x0}^3 d_{y0} d_{z0}} & \frac{C_p}{d_{x0}^2 d_{y0}^2 d_{z0}} & \frac{C_p}{d_{x0}^2 d_{y0} d_{z0}^2} \\ \frac{C_p}{d_{x0}^2 d_{y0}^2 d_{z0}} & \frac{3C_p}{d_{x0} d_{y0}^3 d_{z0}} & \frac{C_p}{d_{x0} d_{y0}^2 d_{z0}^2} \\ \frac{C_p/3}{d_{x0} d_{y0} d_{z0}^2} & \frac{C_p/3}{d_{x0} d_{y0}^2 d_{z0}^2} & \frac{C_p}{d_{x0} d_{y0} d_{z0}^3} + \frac{4}{d_{z0}^4} \end{pmatrix} \begin{pmatrix} \epsilon_x \\ \epsilon_y \\ \epsilon_z \end{pmatrix} \quad (29)$$

Calculating the eigenvalues and eigenfrequencies of the above matrix one finds the collective excitation frequencies and modes. This can be easily done numerically. For simplicity that lends itself to an easy analytical treatment we assume cylindrical symmetry  $\lambda_{x0} = \lambda_{y0} \equiv \lambda_{r0}$ ,  $d_{x0} = d_{y0} \equiv d_{r0}$  and reduce the set of three equations to a set of two

$$\begin{pmatrix} \ddot{\epsilon}_r \\ \ddot{\epsilon}_z \end{pmatrix} = - \begin{pmatrix} 4 & Dd_{z0} \\ \frac{2}{3}Dd_{z0} & 4\lambda_{z0}^2 - \frac{1}{3}Dd_{r0} \end{pmatrix} \begin{pmatrix} \epsilon_r \\ \epsilon_z \end{pmatrix}, \quad (30)$$

where  $D = C_p/(d_{r0}^3 d_{z0}^3)$ . We can diagonalize the above matrix and find the eigenvalues which yields for the eigenfrequencies  $\omega^2$ :

$$\begin{aligned} \frac{\omega^2}{\omega_0^2} &= 2\lambda_{z0}^2 - \frac{1}{6}Dd_{r0} + 2 \\ &\pm \sqrt{\left(-2\lambda_{z0}^2 + \frac{1}{6}Dd_{r0} + 2\right)^2 + \frac{2}{3}D^2 d_{z0}^2}. \end{aligned} \quad (31)$$

Inserting expression (15,17) for the ground state widths into the equation above we obtain an analytic expression for the collective excitation frequencies in the Q2D regime:

$$\begin{aligned} \frac{\omega^2}{\omega_0^2} &= 2\lambda_{z0}^2 - \frac{1}{6}\sqrt{\frac{C_p \lambda_{r0}^2}{\lambda_{z0}^{\frac{5}{2}}}} + 2 \\ &\pm \sqrt{\left(-2\lambda_{z0}^2 + \frac{1}{6}\sqrt{\frac{C_p \lambda_{r0}^2}{\lambda_{z0}^{\frac{5}{2}}}} + 2\right)^2 + \frac{2}{3}\sqrt{C_p \lambda_{r0}^6 \lambda_{z0}^{\frac{5}{2}}}}. \end{aligned}$$

The two frequencies given by Eq.(31) describe the high- and low-lying  $m = 0$  modes of the collective excitation spectrum. The high-lying  $m = 0$  mode is an in-phase compressional mode along all directions (breathing mode). The low-lying  $m = 0$  corresponds to a radial oscillation of the width which is out of phase with an oscillation along the trap axis. The third mode (not described by Eq. 31) in an axially symmetric trap is the  $m = 2$  mode. It corresponds to a quadrupole type excitation in the radial plane and its frequency is given  $\omega_2 = \sqrt{2}\omega_r$ , irrespective of the axial frequency. Fig. 4 shows the change of the collective excitation frequencies of the two  $m = 0$  modes for increasing  $\omega_r$ . We find that the high-lying mode frequency ( $\omega_+$ ) changes from a value of  $\omega_+ = 2\omega_z$  for radial frequencies close to zero to a value of  $\omega_+ = \sqrt{3}\omega_z$  for large radial frequencies. The latter value has been determined from the hydrodynamic model [11], given by the dashed line, in the limit of  $\omega_r \rightarrow 0$ . The hardly distinguishable predictions of the

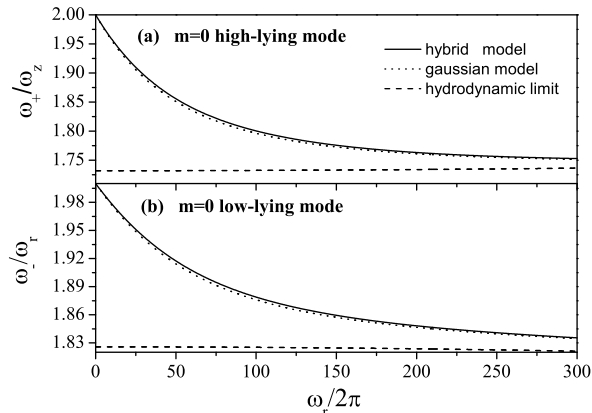


FIG. 4: The  $m = 0$  high-lying mode frequency ( $\omega_+$ ) and the  $m = 0$  low-lying mode frequency ( $\omega_-$ ) plotted against the radial trap frequency  $\omega_r/2\pi$  in figures (a) and (b), respectively; hybrid variational model (solid line), Gaussian variational model (dotted line) and hydrodynamic prediction (dashed line).

hybrid- and Gaussian variational models are given by the solid and dotted lines, respectively. For very small  $\omega_r$ , in the Q2D regime, the mode frequencies approach the ideal or non-interacting gas limit where the mode frequency is twice the trap frequency. In the ideal gas limit the radial oscillation goes towards zero and we obtain a pure axial oscillation for the high-lying mode, which can be found from the eigenvectors of (29).

Something similar happens for the low-lying mode frequency  $\omega_-$  which changes from the hydrodynamic limit of  $\omega_- = \sqrt{10/3} \omega_r$  to  $\omega_- = 2\omega_r$  for decreasing  $\omega_r$ . An analysis of the eigenvector (corresponding to this mode) of matrix (29) shows that in the Q2D regime the axial component of the oscillation is increasingly suppressed and goes towards zero in the limit of infinitely small  $\omega_r$ .

Surprisingly, in this limit the oscillation in the radial direction at the mode frequency  $\omega_- = 2\omega_r$  seems not at all affected by the hydrodynamic character and strong interactions of the gas in the radial plane. It oscillates at the same frequency as an ideal collisionless gas, although it is far from being collisionless. This feature has been pointed out by Pitaevskii and Rosch [13], and depends on the special symmetry in the two-dimensional regime.

## VI. CONCLUSIONS AND OUTLOOK

We studied the properties of Q2D condensates using a hybrid variational model based on a Gaussian-parabolic trial wavefunction. The chemical potential and ground state energy were calculated for a wide range of parameters from the hydrodynamic to the Q2D regime. We find that the chemical potential approaches the harmonic oscillator ground state and derive an analytical expression for its values in the Q2D regime. The condensate size in time-of-flight and its release energy are plotted for traps with varying anisotropy. We find good agreement to recent experimental results [4]. We also calculate the excitation spectrum of the quadrupole modes of the Q2D gas and find a gradual change from the hydrodynamic values to values equal to twice the trap frequencies in the Q2D regime, as predicted in [13]. All results from the hybrid model are compared to those derived from a Gaussian variational model [9], a hydrodynamic model [12] and the ideal gas model. In future work we want to explore the effect Q2D has on vortex structure, dynamics and decay.

## Acknowledgments

The authors would like to acknowledge financial support from the EPSRC and DARPA.

- 
- [1] B. Paredes, A. Widera, V. Murg, O. Mandel, S. Fölling, I. Cirac, G. Shlyapnikov, T. Hansch, and I. Bloch, *NATURE* **429**, 277 (2004).
  - [2] A. Gorlitz, J. Vogels, A. Leanhardt, C. Raman, T. Gustavson, J. Abo-Shaeer, A. Chikkatur, S. Gupta, S. Inouye, T. Rosenband, et al., *Phys. Rev. Lett.* **87** (2001).
  - [3] D. Rychtarik, B. Engeser, H.-C. Nagerl, and R. Grimm, *Phys. Rev. Lett.* **92** (2004).
  - [4] N. L. Smith, W. Heathcote, G. Hechenblaikner, E. Nugent, and C. J. Foot, *cond-mat/0410101* (2004).
  - [5] D. Bishop and D. Reppy, *Phys. Rev. Lett.* **40**, 1727 (1978).
  - [6] J. Kosterlitz and D. Thouless, *J. Phys. C* **6**, 1181 (1973).
  - [7] A. Safonov, S. Vasilyev, I. Yasnikov, I. Lukashevich, and S. Jaakkola, *Phys. Rev. Lett.* **81**, 4545 (1998).
  - [8] K. K. Das, *Phys. Rev. A* **66**, 053612 (2002).
  - [9] V. Perez-Garcia, H. Michinel, J. Cirac, M. Lewenstein, and P. Zoller, *Phys. Rev. Lett.* **77**, 5320 (1996).
  - [10] S. Stringari, *Phys. Rev. Lett.* **77**, 2360 (1996).
  - [11] F. Dalfovo, S. Giorgini, L. P. Pitaevskii, and S. Stringari, *Rev. Mod. Phys.* **71**, 463 (1999).
  - [12] Y. Castin and R. Dum, *Phys. Rev. Lett.* **77**, 5315 (1996).
  - [13] L. Pitaevskii and A. Rosch, *Phys. Rev. A* **55**, R853 (1997).